



## WAMS-based monitoring and control of Hopf bifurcations in multi-machine power systems\*

Shao-bu WANG<sup>†</sup>, Quan-yuan JIANG, Yi-jia CAO<sup>†‡</sup>

(School of Electrical Engineering, Zhejiang University, Hangzhou 310027, China)

<sup>†</sup>E-mail: wangshaobu@yahoo.com.cn; yijiacao@zju.edu.cn

Received Sept. 21, 2007; revision accepted Dec. 25, 2007; published online May 9, 2008

**Abstract:** A method is proposed to monitor and control Hopf bifurcations in multi-machine power systems using the information from wide area measurement systems (WAMSs). The power method (PM) is adopted to compute the pair of conjugate eigenvalues with the algebraically largest real part and the corresponding eigenvectors of the Jacobian matrix of a power system. The distance between the current equilibrium point and the Hopf bifurcation set can be monitored dynamically by computing the pair of conjugate eigenvalues. When the current equilibrium point is close to the Hopf bifurcation set, the approximate normal vector to the Hopf bifurcation set is computed and used as a direction to regulate control parameters to avoid a Hopf bifurcation in the power system described by differential algebraic equations (DAEs). The validity of the proposed method is demonstrated by regulating the reactive power loads in a 14-bus power system.

**Key words:** Wide area measurement system (WAMS), Hopf bifurcations, Monitoring of bifurcations, Control of bifurcations  
**doi:**10.1631/jzus.A0720006 **Document code:** A **CLC number:** TM761; TN751.3

### INTRODUCTION

Along with the continuous extension of the scale of power systems, the dynamic characteristics of power systems become more and more complicated. Moreover, economic and environmental pressures are causing power systems to be operated close to their limits of stability. As a result, some nonlinear singularity phenomena are observed frequently in modern power systems. One of the more prominent examples is the 0.7 Hz sustained oscillation that arises in the Western Systems Coordinating Council (WSCC) following the loss of the AC or DC interties between the Pacific Northwest and California (Mensour, 1990). Sustained oscillations can also arise during the 'normal' steady-state operation (Jiang *et al.*, 1997). The mechanism of these equal amplitude oscillations

has been found associated with the Hopf bifurcation which is featured with a pair of conjugate eigenvalues of the Jacobian matrix of a system crossing the imaginary axis and the trajectory of the system tending to a limit cycle (Ajarapu and Lee, 1992; Wang *et al.*, 1996). Further studies are developed by Dobson *et al.* (1992). In their paper, with loads being considered as parameters in an ODEs (ordinary differential equations) system, a method was presented to increase the loading margin according to the sensitivity of the Hopf bifurcation under the condition that the direction of the increasing loads is known, which will postpone the Hopf bifurcation. In order to describe the dynamical process of power systems in more detail, Lerm *et al.* extended the above work to DAEs (differential algebraic equations) systems (Lerm, 2001; 2002; Lerm and Silva, 2004).

The emerging of wide area measurement systems (WAMSs) offers new opportunities for the monitoring and control of power systems. With WAMS, most state variables and all the algebraic variables of power systems can be obtained directly.

<sup>‡</sup> Corresponding author

\* Project supported by the National Natural Science Foundation of China (Nos. 50595414 and 50507018), the National Key Technologies Supporting Program of China during the 11th Five-Year Plan Period (No. 2006BAA02A01), and the Key Grant Project of MOE, China (No. 305008)

As a result, the location of the current equilibrium point in a power system can be obtained expediently. This paper discusses the monitoring and control of Hopf bifurcations in power systems using the information from WAMS. The current paper is organized as follows. Section 2 presents some concepts about Hopf bifurcations in ODEs systems. Section 3 discusses Hopf bifurcations in power systems based on DAEs. It is discussed in Section 4 using the information from WAMS to monitor Hopf bifurcations in power systems. In Section 5 a method to control Hopf bifurcations in power systems is proposed. Then a 14-bus power system is studied as a case in Section 6. Finally some main conclusions are drawn for this study in Section 7.

## HOPF BIFURCATIONS IN ODES SYSTEMS

This section introduces some basic concepts about bifurcations of ODEs systems. The standard bifurcation theory arises from the study of the stability of ODEs systems (Kuznetsov, 2004). In essence, bifurcations are the changes of the topology of a system caused by the changes of parameters of the system. There are several types of bifurcations in ODEs systems, such as saddle-node bifurcations and Hopf bifurcations. This paper concentrates only on the local bifurcations, especially the local Hopf bifurcations. In a supercritical local Hopf bifurcation, the changes of parameters of the system cause a pair of conjugate eigenvalues of the Jacobian matrix of the system crossing the imaginary axis and the trajectory of the system tending to a limit cycle.

### Bifurcation set in multidimensional parameter space

Consider a system modeled by smoothly parameterized ODEs:

$$\dot{\mathbf{x}} = \mathbf{f}(\mathbf{x}, \boldsymbol{\lambda}), \quad \mathbf{x} \in \mathbb{R}^n, \quad \boldsymbol{\lambda} \in \mathbb{R}^m, \quad m > 2. \quad (1)$$

Assume that when  $\boldsymbol{\lambda}=\boldsymbol{\lambda}_0$  and  $\mathbf{x}=\mathbf{x}_0$ , the system Eq.(1) is asymptotically stable at the point  $(\mathbf{x}_0, \boldsymbol{\lambda}_0)$ . As  $\boldsymbol{\lambda}$  varies in the parameter space  $\mathbb{R}^m$ ,  $\mathbf{x}$  varies in the state space  $\mathbb{R}^n$ . Suppose as  $\boldsymbol{\lambda}$  varies along a certain direction in the parameter space from  $\boldsymbol{\lambda}=\boldsymbol{\lambda}_0$  to  $\boldsymbol{\lambda}=\boldsymbol{\lambda}_*$ ,  $\mathbf{x}$  varies from  $\mathbf{x}=\mathbf{x}_0$  to  $\mathbf{x}=\mathbf{x}_*$  in the state space, and the system Eq.(1) can

keep asymptotically stable when the operating point changes from  $(\mathbf{x}_0, \boldsymbol{\lambda}_0)$  to  $(\mathbf{x}_*, \boldsymbol{\lambda}_*)$ . If  $\boldsymbol{\lambda}$  continues to vary along the direction, the system cannot remain asymptotically stable any more (may become oscillatory or lose stability suddenly) when  $\boldsymbol{\lambda}$  passes across the point  $\boldsymbol{\lambda}_*$ . Then  $(\mathbf{x}_*, \boldsymbol{\lambda}_*)$  is called a bifurcation point of the system Eq.(1), and  $\boldsymbol{\lambda}_*$  is called a bifurcation point in the parameter space. In parameter space, all the bifurcation points constitute a set  $\Sigma$ , and  $\boldsymbol{\lambda}_* \in \Sigma$ .  $\mathbb{R}^m$  is called a multidimensional parameter space when  $m > 2$ , and the set  $\Sigma \subset \mathbb{R}^m$  is typically in the form of surfaces or hypersurfaces in  $\mathbb{R}^m$  and their intersections (Dobson, 1992).

### Normal vectors to Hopf bifurcation set

**Lemma 1** (Dobson, 1993) Suppose the system Eq.(1) has a Hopf bifurcation at  $(\mathbf{x}_*, \boldsymbol{\lambda}_*)$  with  $\mathbf{D}_{\mathbf{x}}\mathbf{f}(\mathbf{x}_*, \boldsymbol{\lambda}_*)$  having a pair of conjugate eigenvalues  $\pm j\omega_*$ ,  $\omega_* \neq 0$  and all other eigenvalues with nonzero real part and satisfying the transversality conditions  $\mathbf{D}_{\boldsymbol{\lambda}}(\text{Re}\{\mu(\boldsymbol{\lambda})\}) \neq 0$  and  $c \neq 0$ , where  $c$  is a coefficient of cubic terms in the flow reduced to the center manifold and is a complicated function of triple derivatives of the function  $\mathbf{f}$ , and  $\mu$  is a smooth function defined in a neighborhood of  $\boldsymbol{\lambda}_*$  with  $\mu(\boldsymbol{\lambda}_*) = j\omega_*$ . Write  $\Sigma^{\text{Hopf}}$  for the Hopf bifurcation set of the system Eq.(1) and  $\mathbf{d}_*$ ,  $\mathbf{e}_*$  for the normalized left and right eigenvectors respectively corresponding to one of the pair of conjugate eigenvalues, then there is an open set  $U$  ( $\boldsymbol{\lambda}_* \in U$ ) such that  $S = \Sigma^{\text{Hopf}} \cap U$  is a smooth hypersurface and the normal vector to  $S$  at  $\boldsymbol{\lambda}_*$  is

$$\mathbf{N}(\boldsymbol{\lambda}_*) = \text{Re}\{\mathbf{d}_*^T (\mathbf{f}_{\mathbf{xx}} \mathbf{U}_{\boldsymbol{\lambda}} + \mathbf{f}_{\mathbf{x}\boldsymbol{\lambda}}) \mathbf{e}_*\}, \quad (2)$$

where  $\mathbf{f}_{\mathbf{xx}}$  is an  $n \times n \times n$  tensor,  $\mathbf{f}_{\mathbf{x}\boldsymbol{\lambda}}$  is an  $n \times n \times m$  tensor, and  $\mathbf{U}_{\boldsymbol{\lambda}}$  is an  $n \times m$  Jacobian matrix given by  $\mathbf{f}_{\mathbf{x}} \mathbf{U}_{\boldsymbol{\lambda}} = -\mathbf{f}_{\boldsymbol{\lambda}}$ .

## HOPF BIFURCATIONS IN POWER SYSTEMS

### Modeling of power systems

The model to describe the electromechanical stability of power systems is a DAEs set, in the form:

$$\begin{cases} \dot{\mathbf{x}} = \mathbf{f}(\mathbf{x}, \mathbf{y}, \boldsymbol{\lambda}), \\ \mathbf{0} = \mathbf{g}(\mathbf{x}, \mathbf{y}, \boldsymbol{\lambda}), \end{cases} \quad (3)$$

where  $\mathbf{x}$  is a vector of state variables of a power sys-

tem,  $\mathbf{y}$  is a vector of algebraic variables of a power system, and  $\lambda$  is a vector of parameter variables of a power system,  $\lambda \in \chi$ , where  $\chi$  denotes the space of parameter variables.

**Hopf bifurcations in DAEs systems**

The stability of DAEs systems is studied in detail by Hill and Mareels (1990). The main idea is that if  $D_y \mathbf{g}(\mathbf{x}, \mathbf{y}, \lambda)$  is nonsingular along the system trajectories of interest, the dynamic behavior of the system Eq.(3) along these trajectories is determined by the local ODEs reduction:

$$\dot{\mathbf{x}} = \mathbf{f}(\mathbf{x}, \mathbf{y}^{-1}(\mathbf{x}, \lambda), \lambda), \tag{4}$$

where  $\mathbf{y}=\mathbf{y}^{-1}(\mathbf{x}, \lambda)$  is determined by applying the Implicit Function Theorem to the algebraic equations  $\mathbf{0}=\mathbf{g}(\mathbf{x}, \mathbf{y}, \lambda)$  on the trajectories of interest. The Jacobian matrix of the system Eq.(4) is shown as follows:

$$\mathbf{A} = D_x \mathbf{f} - D_y \mathbf{f} (D_y \mathbf{g})^{-1} D_x \mathbf{g}. \tag{5}$$

So according to the characteristics of Hopf bifurcations, if the system Eq.(3) has a Hopf bifurcation at  $(\mathbf{x}^*, \mathbf{y}^*, \lambda^*)$ , then  $\mathbf{A}$  in Eq.(5) must have a pair of conjugate eigenvalues crossing the imaginary axis.

**Normal vectors to Hopf bifurcation set of DAEs systems**

According to Lemma 1, the normal vector to the Hopf bifurcation set of the system Eq.(3) at  $(\mathbf{x}^*, \mathbf{y}^*, \lambda^*)$  is

$$\mathbf{N}(\lambda^*) = \text{Re} \{ \mathbf{d}^{*T} (\mathbf{A}_x \mathbf{U}_\lambda + \mathbf{A}_z) \mathbf{e}_* \}. \tag{6}$$

Notice that  $\mathbf{A}$  in Eq.(5) contains the term  $(D_y \mathbf{g})^{-1}$ , so it is very difficult to determine  $\mathbf{A}_x$  and  $\mathbf{A}_z$  in Eq.(6). In order to avoid this problem, a method based on “extended” eigenvectors is proposed by Smed (1993). The main idea about “extended” eigenvectors can be stated as

$$\begin{bmatrix} \sigma \mathbf{e}_1 \\ \mathbf{0} \end{bmatrix} = \begin{bmatrix} D_x \mathbf{f} & D_y \mathbf{f} \\ D_x \mathbf{g} & D_y \mathbf{g} \end{bmatrix} \begin{bmatrix} \mathbf{e}_1 \\ \mathbf{e}_2 \end{bmatrix}, \tag{7}$$

where  $\mathbf{e}=[\mathbf{e}_1^T \ \mathbf{e}_2^T]^T$  is the “extended” right eigenvector associated with the eigenvalue  $\sigma$  of  $\mathbf{A}$  in Eq.(5). It is implied in Eq.(7) that

$$\begin{cases} \mathbf{e}_2 = -[(D_y \mathbf{g})^{-1} D_x \mathbf{g}] \mathbf{e}_1, \\ \sigma \mathbf{e}_1 = \mathbf{A} \mathbf{e}_1. \end{cases} \tag{8}$$

Conversely if  $\sigma$ ,  $\mathbf{e}_1$  and  $\mathbf{e}_2$  satisfy Eq.(8), then Eq.(7) can be obtained and the “extended” right eigenvector of the system Eq.(3) can be determined. A similar way can be used to determine the “extended” left eigenvector  $\mathbf{d}=[\mathbf{d}_1^T \ \mathbf{d}_2^T]^T$ .

Using the above method, the normal vector to the Hopf bifurcation set of the system Eq.(3) at  $(\mathbf{x}^*, \mathbf{y}^*, \lambda^*)$  can be written as

$$\mathbf{N}(\lambda^*) = \text{Re} \{ \mathbf{d}^{*T} (\mathbf{F}_{zz} \mathbf{U}_\lambda + \mathbf{F}_{z\lambda}) \mathbf{e}_* \}, \tag{9}$$

where  $\mathbf{F}=[\mathbf{f}, \mathbf{g}]^T$  and  $\mathbf{z}=[\mathbf{x}, \mathbf{y}]^T$ , the eigenvectors  $\mathbf{d}^*$  and  $\mathbf{e}^*$  in Eq.(9) can be determined by solving Eq.(8) in which  $\sigma$  can be any one of the pair of conjugate eigenvalues,  $\mathbf{U}_\lambda$  can be obtained by solving  $\mathbf{F}_z \mathbf{U}_\lambda = -\mathbf{F}_\lambda$ .

**MONITORING OF HOPF BIFURCATIONS WITH INFORMATION FROM WAMS**

According to Part 2 of Section 3, if there is a Hopf bifurcation in the system Eq.(3),  $\mathbf{A}$  in Eq.(5) must have a pair of conjugate eigenvalues crossing the imaginary axis. So the distance between the current equilibrium point and the Hopf bifurcation set can be obtained by computing the eigenvalues of  $\mathbf{A}$ . A method using the information from WAMS to monitor Hopf bifurcations in power systems is discussed thoroughly in this section.

**Determining the location of the current equilibrium point**

In power systems, most state variables and all the algebraic variables in Eq.(3) can be obtained directly from WAMS except some state variables that cannot be measured directly, such as  $E_q''$  and  $E_d''$ . So with WAMS, the location of the current equilibrium point can be obtained by solving only the subset of Eq.(10) corresponding to the state variables that cannot be measured directly.

$$\begin{cases} \mathbf{0} = \mathbf{f}(\mathbf{x}, \mathbf{y}, \lambda), \\ \mathbf{0} = \mathbf{g}(\mathbf{x}, \mathbf{y}, \lambda). \end{cases} \tag{10}$$

As a result, the number of the equations needed to be solved to determine an equilibrium point decreases greatly. This means that with the information from WAMS, the location of the current equilibrium point can be obtained quickly and accurately and then  $A$  can be obtained easily. Then by computing the eigenvalues of  $A$ , the distance between the current equilibrium point and the Hopf bifurcation set can be monitored dynamically.

**Monitoring of Hopf bifurcations**

According to the distribution of the eigenvalues of  $A$ , information about the Hopf bifurcation of the system Eq.(3) can be obtained expediently. But it is time-consuming to compute all the eigenvalues of  $A$ , especially when the order of  $A$  is high. In order to avoid computing all the eigenvalues, an algorithm is adopted to compute only the pair of conjugate eigenvalues with the algebraically largest real part. The algorithm can be stated as follows. Let

$$Z = (A + I)(A - I)^{-1}, \tag{11}$$

where  $I$  is an identity matrix, and  $I$  and  $A$  have the same order. Write  $\sigma_A$  for a certain eigenvalue of  $A$  and  $\sigma_Z$  for the corresponding eigenvalue of  $Z$ . Then it can be known from Eq.(11) that  $\sigma_A$  and  $\sigma_Z$  have the same eigenvector and the relationship between  $\sigma_A$  and  $\sigma_Z$  is

$$\sigma_Z = (\sigma_A + 1)/(\sigma_A - 1). \tag{12}$$

In the complex plane, the imaginary axis for  $\sigma_A$  is mapped into a unit circle for  $\sigma_Z$  by Eq.(11). Once the Jacobian matrix  $A$  has a certain eigenvalue crossing the imaginary axis, the matrix  $Z$  must have a corresponding eigenvalue crossing the unit cycle radially. As a result, if the spectral radius  $\rho(Z) < 1$ , then all the eigenvalues of  $A$  are at the left half plane and the system is asymptotically stable; if  $\rho(Z) > 1$ ,  $A$  has a corresponding eigenvalue at the right half plane and the current equilibrium point is unstable; if  $\rho(Z) = 1$ ,  $A$  has a corresponding eigenvalue on the imaginary axis and the current equilibrium point is a bifurcation point. For Hopf bifurcations,  $Z$  has a pair of conjugate eigenvalues crossing the unit circle. This paper adopts the power method (PM) to compute the pair of conjugate eigenvalues with the largest module. The de-

tails about the method are presented in the following subsection.

**Computing the largest module eigenvalues and the corresponding eigenvectors**

In power systems,  $Z$  is a real matrix. So for  $Z$ , the pair of conjugate eigenvalues with the largest module can be computed by the PM, which can be stated as the iterative process shown in Eq.(13):

$$\begin{cases} \mathbf{u}_0 = \mathbf{v}_0, \\ \mathbf{v}_k = Z\mathbf{u}_{k-1}, \\ m_k = \max(|\mathbf{v}_{ki}|), \quad i = 0, 1, 2, \dots, n, \\ \mathbf{u}_k = \mathbf{v}_k / m_k, \end{cases} \tag{13}$$

where  $\mathbf{v}_0$  is a random  $n$ -dimensional real vector,  $m_k$  is the largest module of the components of the vector  $\mathbf{v}_k$ .

Write  $\sigma_{Z1}$  and  $\sigma_{Z2}$  for the pair of conjugate eigenvalues with the largest module,  $\sigma_{Z1} = (\sigma_{Z2})^*$ ,  $|\sigma_{Z1}| = |\sigma_{Z2}|$ . According to the PM, we have

$$Z^{k+2}\mathbf{u}_0 + pZ^{k+1}\mathbf{u}_0 + qZ^k\mathbf{u}_0 \rightarrow 0, \quad (k \rightarrow \infty), \tag{14}$$

where  $p = -(\sigma_{Z1} + \sigma_{Z2})$  and  $q = \sigma_{Z1}\sigma_{Z2}$ . It follows from Eqs.(13) and (14) that

$$m_{k+1}m_{k+2}\mathbf{u}_{k+2} + pm_{k+1}\mathbf{u}_{k+1} + q\mathbf{u}_k \rightarrow 0, \quad (k \rightarrow \infty). \tag{15}$$

Using the least squares method to deal with the over-determined Eq.(15), we can obtain  $p$  and  $q$  as follows:

$$\begin{aligned} p^k &= -m_{k+2} \left( \mathbf{u}_{k+1}^T \mathbf{u}_{k+2} \mathbf{u}_k^T \mathbf{u}_k - \mathbf{u}_k^T \mathbf{u}_{k+1} \mathbf{u}_k^T \mathbf{u}_{k+2} \right) \\ &\quad \cdot \left[ \mathbf{u}_{k+1}^T \mathbf{u}_{k+1} \mathbf{u}_k^T \mathbf{u}_k - (\mathbf{u}_k^T \mathbf{u}_{k+1})^2 \right]^{-1}, \\ q^k &= -m_{k+1}m_{k+2} \left( \mathbf{u}_{k+1}^T \mathbf{u}_{k+1} \mathbf{u}_k^T \mathbf{u}_{k+2} - \mathbf{u}_k^T \mathbf{u}_{k+1} \mathbf{u}_k^T \mathbf{u}_{k+2} \right) \\ &\quad \cdot \left[ \mathbf{u}_{k+1}^T \mathbf{u}_{k+1} \mathbf{u}_k^T \mathbf{u}_k - (\mathbf{u}_k^T \mathbf{u}_{k+1})^2 \right]^{-1}. \end{aligned}$$

When  $|p^k - p^{k-1}| < \varepsilon$  or  $|q^k - q^{k-1}| < \varepsilon$  ( $\varepsilon$  is a given tolerance), the iterative process Eq.(13) can be broken. Then the pair of conjugate eigenvalues can be obtained and given as

$$\sigma_{Z1,2}^k \approx \frac{1}{2} \left( -p^k \pm j\sqrt{4q^k - (p^k)^2} \right). \tag{16}$$

The eigenvectors corresponding to the pair of conjugate eigenvalues  $\sigma_{Z1}$  and  $\sigma_{Z2}$ , respectively, are

$$v_{Z1} \approx [(u^{k+2} - \sigma_{Z1r} u^{k+2}) + j\sigma_{Z1i} u^{k+1}] / \rho, \quad (17)$$

$$v_{Z2} = \bar{v}_{Z1} \approx [(u^{k+2} - \sigma_{Z1r} u^{k+2}) - j\sigma_{Z1i} u^{k+1}] / \rho, \quad (18)$$

where  $\rho = \|u^{k+2} - \sigma_{Z1} u^{k+1}\|$ ,  $\sigma_{Z1r}$  and  $\sigma_{Z1i}$  are the real and imaginary parts of  $\sigma_{Z1}$ , respectively.

The eigenvalue  $\sigma_{A1}$  corresponding to  $\sigma_{Z1}$  can be obtained by solving Eq.(12). Notice that  $v_{Z1}$  and  $v_{Z2}$  are also the eigenvectors of  $\sigma_{A1}$  and  $\sigma_{A2}$ , respectively. The corresponding left eigenvectors can be obtained in a similar way.

**Monitoring flowchart**

The flowchart in Fig.1 describes the steps involved for the monitoring of Hopf bifurcations in power systems with the information from WAMS.

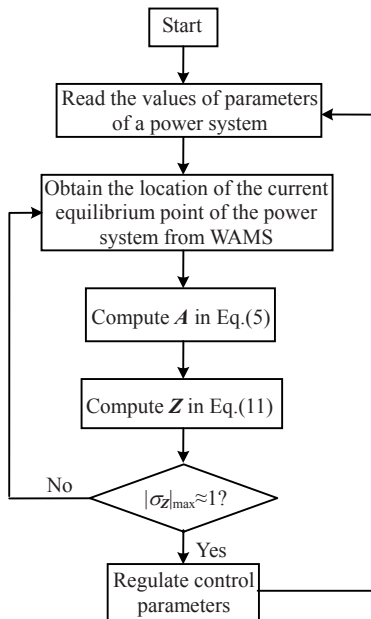


**Fig.1 Flowchart for monitoring of Hopf bifurcations with the information from WAMS**

Step 1: Read the values of parameters of a power system from the database of the power system;

Step 2: Obtain the location of the current equilibrium point of the power system from WAMS.

Step 3: Compute  $A$  and  $Z$ . Then the PM is used to compute the largest module conjugate eigenvalues of  $Z$ .

Step 4: Judge whether the largest module conjugate eigenvalues are close to the unit circle. If the

largest module conjugate eigenvalues are close to the unit circle, then regulate the control parameters to avoid a Hopf bifurcation and return to Step 1; else return to Step 2.

**CONTROL OF HOPF BIFURCATIONS**

**Approximate normal vectors to Hopf bifurcation set**

The concept of the approximate normal vector to the saddle-node bifurcation set of ODEs systems is mentioned by Dobson and Lu (1993). In this paper we extend the idea to the Hopf bifurcation set of ODEs systems. The main idea about the approximate normal vector to the Hopf bifurcation set can be illustrated in a sketch map of a two-parameter space as shown in Fig.2.

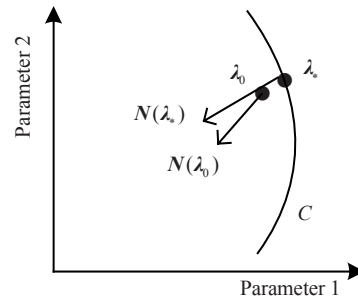


**Fig.2 Sketch map of a two-parameter space**

Suppose  $(x_0, \lambda_0)$  is an equilibrium point of the system Eq.(1) and  $\sigma_{A1,2}$  are the pair of conjugate eigenvalues with the algebraically largest real part of the Jacobian matrix of the system,  $e_0$  and  $d_0$  are the right and left eigenvectors corresponding to  $\sigma_{A1}$ , respectively. In Fig.2,  $\lambda_0$  is a point in the parameter space and the curve  $C$  is the bifurcation set. For multidimensional parameter space, the bifurcation set is in the form of surfaces or hypersurfaces. Along with  $\lambda_0$  approaches the bifurcation set in the parameter space,  $\sigma_{A1,2}$  approach the imaginary axis in the complex plane. When  $\lambda_0$  is close enough to the bifurcation set, suppose in the bifurcation set  $\lambda_*$  is the closest point to the point  $\lambda_0$ , then the normal vector  $N(\lambda_*)$  can be approximated by the direction of  $N(\lambda_0)$  as shown in Fig.2. The direction of  $N(\lambda_0)$  can be computed by substituting  $e_0$  and  $d_0$  for  $e_*$  and  $d_*$  in Eq.(2), respectively. Then Eq.(19) can be obtained:

$$N(\lambda_0) = \text{Re} \{ d_0^T (f_{xx} U_\lambda + f_{x\lambda}) e_0 \}. \quad (19)$$



Now we extend the above idea further to the Hopf bifurcation set of DAEs systems and use the PM to compute the approximate normal vector to the Hopf bifurcation set. According to the results of monitoring of Hopf bifurcations, when  $\sigma_{z1,2}$  in Eq.(16) are close to the unit circle, the approximate normal vector to the Hopf bifurcation set at  $(x_0, y_0, \lambda_0)$  can be computed as follows:

(1) Compute the pair of conjugate eigenvalues  $\sigma_{A1,2}$  with the algebraically largest real part by solving Eq.(12);

(2) In Eq.(8), let  $\sigma = \sigma_{A1}$  and substitute  $v_{z1}$  from Eq.(17) for  $e_1$ . Then compute  $e_2$  by solving Eq.(8), and thus the "extended" right eigenvector  $e_0 = [e_1^T e_2^T]^T$  can be obtained;

(3) Compute the "extended" left eigenvector  $d_0 = [d_1^T d_2^T]^T$  in a similar way;

(4) According to Eqs.(9) and (19), the approximate normal eigenvector to the Hopf bifurcation set at the current equilibrium point  $(x_0, y_0, \lambda_0)$  can be obtained and given as

$$N(\lambda_0) = \text{Re} \left\{ d_0^T (F_{zz} U_\lambda + F_{z\lambda}) e_0 \right\}. \quad (20)$$

### Control of Hopf bifurcations

When the current equilibrium point is close to the Hopf bifurcation set, choose those parameters that can be regulated expediently and compute the approximate normal vector to the Hopf bifurcation set using Eq.(20) in the chosen parameter space. And then according to the approximate normal vector, regulate the control parameters to decrease the real part of the pair of conjugate eigenvalues so as to avoid the Hopf bifurcation. Those parameters easy to be regulated can be chosen to form a subspace called control parameter space, denoted by  $\chi_c$  in this paper, and  $\chi_c \subset \chi$ . In power systems, many load nodes are equipped with compensation devices in order to optimize the distribution of reactive power. So the reactive power loads can be regulated expediently. We choose the reactive power loads as control parameters. Notice that the changes of the control parameters will cause the changes of the power flow distribution at the same time. So it is vital to choose an appropriate step  $k$  in Eq.(21) for the control of Hopf bifurcations in power systems:

$$\lambda_c = \lambda_{c0} + kN(\lambda_{c0}), \quad \lambda_c \in \chi_c. \quad (21)$$

The direction and amplitude of  $k$  have to satisfy:

- (1) The real part of the pair of conjugate eigenvalues is on the decrease;
- (2) The power flow is feasible.

## CASE STUDY

### Numerical example

In this section, we apply the method presented above to analyze the IEEE 14-bus system. The structure of the grid is shown in Fig.3.

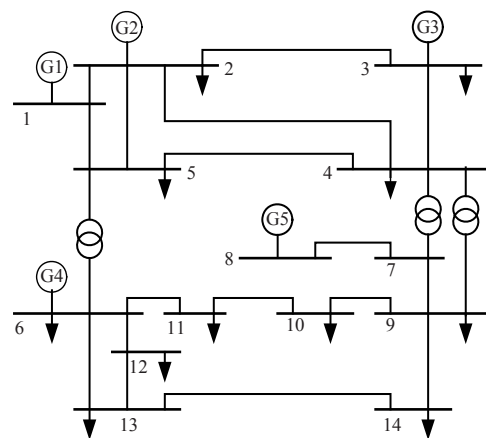


Fig.3 Structure of the IEEE 14-bus system with 14 buses (1~14) and 5 machines (G1~G5)

There are five machines in the system. The 5th-order model in the variables  $\delta, \omega, E_q', E_q''$  and  $E_d''$  is adopted for G1 and the 6th-order model in the variables  $\delta, \omega, E_q', E_d', E_q''$  and  $E_d''$  for the others. All five machines are with AVRs (automatic voltage regulators) described by the 4th-order model in the state variables  $v_m, v_{r1}, v_{r2}$  and  $v_f$ . The whole system is a 48th-order system except a redundant state variable. The parameters of the machines and AVRs are given in Tables 1 and 2, respectively, and the loads of the system are given in Table 3. All loads are considered independent on the voltage for both active and reactive power. All the reactive power loads in the system can be regulated and are chosen to form the control parameter space. In Tables 1~3, all the parameters are obtained under the condition that the base power is 100 MW and the base frequency is 60 Hz.

Choose G1 as the reference machine to eliminate the redundant state variable. At the equilibrium point  $(x_0, y_0, \lambda_0)$  corresponding to Table 3, after 291

**Table 1 Dynamic parameters of machines in the example case system**

Parameter	Unit	G1	G2	G3	G4	G5
Leakage reactance $x_l$	p.u.	0.2396	0	0	0.1340	0.1340
Armature resistance $r_a$	p.u.	0	0.0031	0.0031	0.0014	0.0014
$d$ -axis synchronous reactance $x_d$	p.u.	0.8979	1.0500	1.0500	1.2500	1.2500
$d$ -axis transient reactance $x_d'$	p.u.	0.640	0.185	0.185	0.232	0.232
$d$ -axis subtransient reactance $x_d''$	p.u.	0.23	0.13	0.13	0.12	0.12
$d$ -axis open circuit transient time constant $T'_{d0}$	s	7.40	6.10	6.10	4.75	4.75
$d$ -axis open circuit subtransient time constant $T''_{d0}$	s	0.03	0.04	0.04	0.06	0.06
$q$ -axis synchronous reactance $x_q$	p.u.	0.646	0.980	0.980	1.220	1.220
$q$ -axis transient reactance $x_q'$	p.u.	0.646	0.360	0.360	0.715	0.715
$q$ -axis subtransient reactance $x_q''$	p.u.	0.40	0.13	0.13	0.12	0.12
$q$ -axis open circuit transient time constant $T'_{q0}$	s	0	0.3	0.3	1.5	1.5
$q$ -axis open circuit subtransient time constant $T''_{q0}$	s	0.033	0.099	0.099	0.210	0.210
Mechanical starting time $M$	kW·s/(kV·A)	10.296	13.080	13.080	10.120	10.120
Damping coefficient $D$	p.u.	2	2	2	2	2
Active power ratio at node $\gamma_P^*$		1	1	1	1	1
Reactive power ratio at node $\gamma_Q^{**}$		1	1	1	1	1

\*  $\gamma_P \in [0, 1]$ ; \*\*  $\gamma_Q \in [0, 1]$

**Table 2 Dynamic parameters of AVRs in the example case system**

Parameter	Unit	AVR 1	AVR 2	AVR 3	AVR 4	AVR 5
Maximum regulator voltage $V_{rmax}$	p.u.	7.32	4.38	4.38	6.81	6.81
Minimum regulator voltage $V_{rmin}$	p.u.	0	0	0	1.395	1.395
Regulator gain $\mu_0$	p.u.	200	20	20	20	20
1st pole $T_1$	s	0.02	0.02	0.02	0.02	0.02
1st zero $T_2$	s	0.002	0.001	0.001	0.001	0.001
2nd pole $T_3$	s	1	1	1	1	1
2nd zero $T_4$	s	0.01	0.01	0.01	0.01	0.01
Field circuit time constant $T_e$	p.u.	0.20	1.98	1.98	0.70	0.70
Measurement time constant $T_r$	p.u.	0.001	0.001	0.001	0.001	0.001
1st ceiling coefficient $A_e$	–	0.0006	0.0006	0.0006	0.0006	0.0006
2nd ceiling coefficient $B_e$	–	0.9	0.9	0.9	0.9	0.9

**Table 3 Load distribution in the example case system**

Load	Unit	Bus 2	Bus 3	Bus 4	Bus 5	Bus 6	Bus 9	Bus 10	Bus 11	Bus 12	Bus 13	Bus 14
$P$	p.u.	0.2597	1.1276	0.5722	0.0910	0.1341	0.3531	0.1077	0.1077	0.0730	0.1616	0.1784
$Q$	p.u.	0.4729	0.7076	0.1490	0.0596	0.2793	0.6182	0.2160	0.0670	0.0596	0.2160	0.1862

iterations under the condition that the tolerance  $\varepsilon=10^{-5}$ , the pair of conjugate eigenvalues with the largest module of  $Z$  is obtained and given as  $\sigma_{0Z1,2}=0.9779 \pm 0.2218j$ . By solving Eq.(12), the corresponding pair of conjugate eigenvalues of  $A$  is obtained and given as  $\sigma_{0A1,2}=0.1104 \pm 8.9285j$ . At the equilibrium point  $(x_0, y_0, \lambda_0)$ , a three-phase fault  $x_f=0.2$  p.u. is applied at Bus 9 on the line 9-10 and cleared after 50 ms. After the system is disturbed, the oscillation of  $\delta_2$  is shown in Fig.4a. And Fig.4b shows the trajectory of the system.

It can be seen from Fig.4a that the disturbance has caused the equal amplitude oscillation of  $\delta_2$ . Fig.4b shows that the trajectory of the system tends to a limit cycle. From Fig.4, it can be inferred that a supercritical Hopf bifurcation has taken place before the equilibrium point reaches the current equilibrium point. Notice that the current equilibrium point is an unstable equilibrium point, not the Hopf bifurcation point, which is the equilibrium point that corresponds to the tiny neighborhood around zero of the real part of the conjugate eigenvalues of  $A$ .

Using the process mentioned in Section 5, the approximate normal vector  $N(\lambda_{c0})$  at the current equilibrium point can be obtained as [0.2801, 0.0811, 0.5043, 0.4373, 0.2101, -0.0075, 0.2370, 0.4737, 0.7738, 0.5064, 0.5097], corresponding to the vector of control parameters  $[Q_2, Q_3, Q_4, Q_5, Q_6, Q_9, Q_{10}, Q_{11}, Q_{12}, Q_{13}, Q_{14}]$ . Now we regulate the control parameters in the control parameter space according to the approximate normal vector  $N(\lambda_{c0})$ . When  $k=-0.5$  in Eq.(21), the equilibrium point of the system varies from  $(x_0, y_0, \lambda_0)$  to  $(x, y, \lambda)$ , the pair of conjugate eigenvalues of  $Z$  varies from  $\sigma_{0Z1,2}=0.9779\pm 0.2218j$  to  $\sigma_{Z1,2}=0.9706\pm 0.2201j$ , and the corresponding variation of the pair of conjugate eigenvalues of  $A$  is from  $\sigma_{0A1,2}=0.1104\pm 8.9285j$  to  $\sigma_{A1,2}=-0.1908\pm 8.9271j$ . At the equilibrium point  $(x, y, \lambda)$ , after the system is disturbed by the same disturbance as above, the damped oscillation of  $\delta_2$  is shown in Fig.5a, and the corresponding trajectory of the system is shown in

Fig.5b. It can be seen from Fig.5 that the oscillation can calm down after about 15 s. So the point  $(x, y, \lambda)$  can satisfy the requirement of the practical small signal stability region. If  $k$  continues to decrease, the real part of the pair of conjugate eigenvalues, i.e.  $\text{Re}(\sigma_{A1,2})$ , will decrease further, but the power flow will become infeasible when  $k$  is small enough.

**Results analysis**

It can be seen from Fig.2 that the normal vector is the optimal direction to regulate control parameters to avoid a bifurcation. But in fact, to regulate control parameters along any direction which is not orthogonal to the normal vector in parameter space will cause the changes of  $\text{Re}(\sigma_{A1,2})$ . In another word, for a given random direction, if along the direction to regulate the control parameters causes  $\text{Re}(\sigma_{A1,2})$  increasing, then along the minus direction to regulate the control parameters will cause  $\text{Re}(\sigma_{A1,2})$

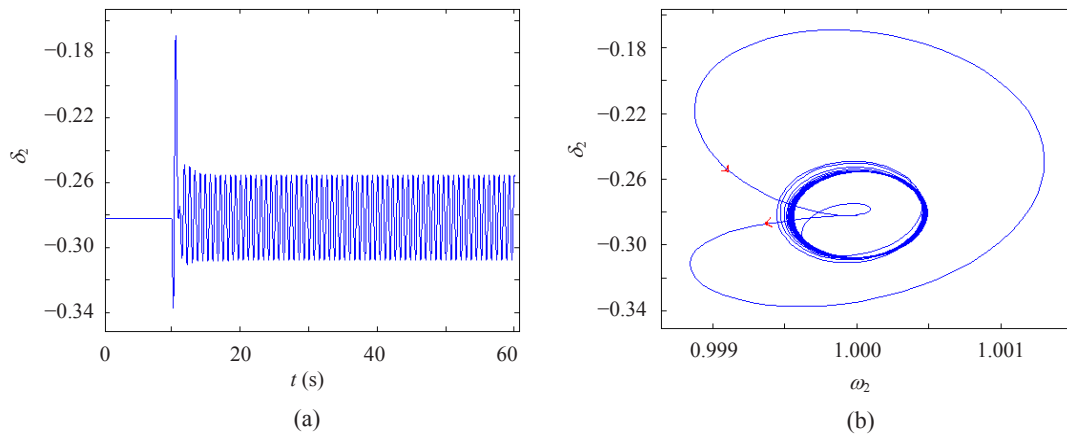


**Fig.4 Sustained oscillation of  $\delta_2$  (a) and the corresponding trajectory in the  $\delta_2$ - $\omega_2$  plane (b) after the system is disturbed at the equilibrium point  $(x_0, y_0, \lambda_0)$**

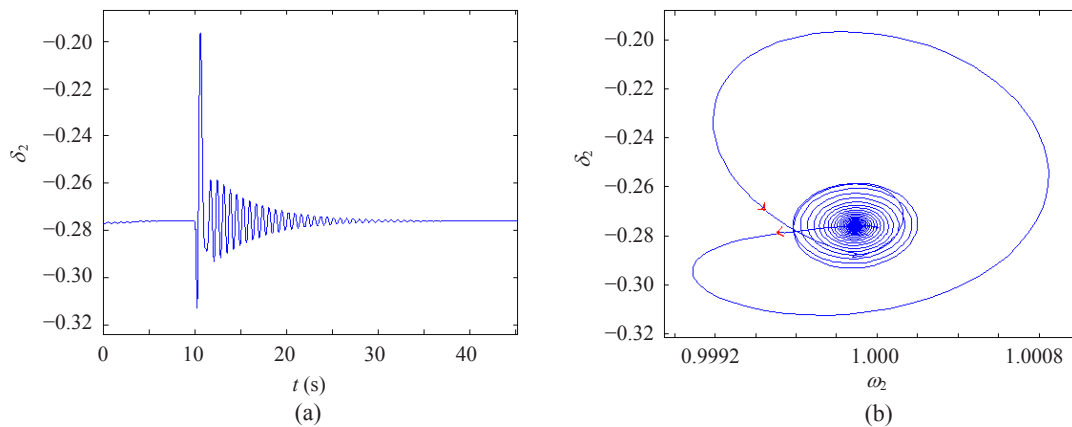


**Fig.5 Damping oscillation of  $\delta_2$  (a) and the corresponding trajectory in the  $\delta_2$ - $\omega_2$  plane (b) after the system is disturbed at the equilibrium point  $(x, y, \lambda)$**



decreasing, which will avoid the Hopf bifurcation also. Whereupon another problem emerges that how to demonstrate the direction obtained in Part 1 of this section is the approximate direction of the normal vector in the control parameter space. We notice that Eq.(2) is essentially the derivatives of  $\text{Re}(\sigma_{A1,2})$  with respect to the control parameters. So the offset of the real part will exceed greatly the offset of the imaginary part when the control parameters vary along the approximate normal vector to the Hopf bifurcation set. In Part 1 of this section, we notice

$$\frac{\text{Re}(\sigma_{0A} - \sigma_A)}{\text{Im}(\sigma_{0A} - \sigma_A)} = \frac{0.1104 + 0.1908}{8.9285 - 8.9271} = 215.14. \quad (22)$$

Eq.(22) suggests that the obtained direction is the approximate normal vector to the Hopf bifurcation set.

## CONCLUSION

With the information from the wide area measurement systems (WAMSs), the distance between the current equilibrium point and the Hopf bifurcation set can be monitored and controlled dynamically by the method proposed in this paper. The power method (PM) is adopted to compute only the pair of conjugate eigenvalues with the algebraically largest real part of the Jacobian matrix of a power system, which makes the monitoring and control of Hopf bifurcations in power systems efficient and time-saving. Therefore, the method is of significance for on-line monitoring and control of Hopf bifurcations in power systems. The validity of the method is demonstrated by numerical results of a 48th-order case. For larger scale power systems, some fast parallel PMs can be adopted to compute the pair of conjugate eigenvalues with the algebraically largest real part and the corresponding eigenvectors.

## References

- Ajjarapu, V., Lee, B., 1992. Bifurcation theory and its application to nonlinear dynamical phenomena in an electrical power. *IEEE Trans. on Power Syst.*, **7**(1):424-431. [doi:10.1109/59.141738]
- Dobson, I., 1992. An Iterative Method to Compute a Closest Saddle Node or Hopf Bifurcation Instability in Multidimensional Parameter Space. Proc. IEEE Int. Symp. on Circuits and Systems, p.2513-2516.
- Dobson, I., 1993. Computing a closest bifurcation instability in multidimensional parameter space. *J. Nonl. Sci.*, **3**(1): 307-327. [doi:10.1007/BF02429868]
- Dobson, I., Lu, L., 1993. New methods for computing a closest saddle bifurcation and worst case load power margin for voltage collapse. *IEEE Trans. on Power Syst.*, **8**(3):905-912. [doi:10.1109/59.260912]
- Dobson, I., Alvarado, F., DeMarco, C.L., 1992. Sensitivity of Hopf Bifurcations to Power System Parameters. Proc. 31st IEEE Conf. on Decision and Control. Tucson, Arizona, p.2928-2933. [doi:10.1109/CDC.1992.371275]
- Hill, D.J., Mareels, I.M.Y., 1990. Stability theory for differential/algebraic systems with application to power systems. *IEEE Trans. on Circuits Syst.*, **37**(11):1416-1423. [doi:10.1109/31.62415]
- Jiang, H.B., Cai, H.Z., Dorsey, J.F., 1997. Toward a globally robust decentralized control for large-scale power systems. *IEEE Trans. on Control Syst. Technol.*, **5**(3):309-319. [doi:10.1109/87.572128]
- Kuznetsov, Y.A., 2004. Elements of Applied Bifurcation Theory (3rd Ed.). Springer-Verlag, New York.
- Lerm, A.A.P., 2001. Control of Hopf Bifurcation in Power Systems Via a Generation Redispatch. Proc. IEEE Power Tech. Porto, Portugal, p.1-6.
- Lerm, A.A.P., 2002. Control of Hopf Bifurcation in Multi-Area Power Systems Via a Secondary Voltage Regulation Scheme. IEEE Power Engineering Society Summer Meeting, p.1615-1620. [doi:10.1109/PSS.2002.1043663]
- Lerm, A.A.P., Silva, A.S., 2004. Avoid Hopf bifurcations in power systems via set point tuning. *IEEE Trans. on Power Syst.*, **19**(2):1076-1084. [doi:10.1109/TPWRS.2004.825827]
- Mensour, Y., 1990. Application of Eigenanalysis to the Western North American Power System. Eigenanalysis and Frequency Domain Methods for System Dynamic Performance. IEEE Publication No. 90TH02923-PWR, p.97-104.
- Smed, T., 1993. Feasible eigenvalue sensitivity for large power systems. *IEEE Trans. on Power Syst.*, **8**(2):555-563. [doi:10.1109/59.260827]
- Wang, S., Crouch, P., Armbruster, D., 1996. Bifurcation Analysis of Oscillations in Electric Power Systems. Proc. 35th IEEE Conf. on Decision and Control. Kobe, Japan, p.3864-3869. [doi:10.1109/CDC.1996.577266]